Atmos. Chem. Phys., 12, 7625–7633, 2012
www.atmos-chem-phys.net/12/7625/2012/
doi:10.5194/acp-12-7625-2012

Atmospheric Chemistry and Physics

Brightening of the global cloud field by nitric acid and the associated radiative forcing

R. Makkonen[1,*], S. Romakkaniemi[2], H. Kokkola[3], P. Stier[4], P. Räisänen[5], S. Rast[6], J. Feichter[6], M. Kulmala[1], and A. Laaksonen[2,5]

[1]Department of Physics, P.O. Box 64, 00014 University of Helsinki, Finland
[2]Department of Applied Physics, University of Eastern Finland, P.O. Box 1627, 70211 Kuopio, Finland
[3]Finnish Meteorological Institute, Kuopio Unit, P.O. Box 1627, 70211, Kuopio, Finland
[4]Atmospheric, Oceanic and Planetary Physics, Department of Physics, University of Oxford, Parks Road, Oxford, OX1 3PU, UK
[5]Finnish Meteorological Institute, P.O. Box 503, 00101, Helsinki, Finland
[6]Max Planck Institute for Meteorology, Bundesstr. 53, 20146 Hamburg, Germany
[*]now at: Department of Geosciences, University of Oslo, P.O. Box 1047, 0316 Oslo, Norway

Correspondence to: R. Makkonen (risto.makkonen@helsinki.fi)

Received: 8 February 2012 – Published in Atmos. Chem. Phys. Discuss.: 17 February 2012
Revised: 2 August 2012 – Accepted: 14 August 2012 – Published: 22 August 2012

Abstract. Clouds cool Earth's climate by reflecting 20 % of the incoming solar energy, while also trapping part of the outgoing radiation. The effect of human activities on clouds is poorly understood, but the present-day anthropogenic cooling via changes of cloud albedo and lifetime could be of the same order as warming from anthropogenic addition in CO_2. Soluble trace gases can increase water condensation to particles, possibly leading to activation of smaller aerosols and more numerous cloud droplets. We have studied the effect of nitric acid on the aerosol indirect effect with the global aerosol-climate model ECHAM5.5-HAM2. Including the nitric acid effect in the model increases cloud droplet number concentrations globally by 7 %. The nitric acid contribution to the present-day cloud albedo effect was found to be $-0.32\,\mathrm{W\,m^{-2}}$ and to the total indirect effect $-0.46\,\mathrm{W\,m^{-2}}$. The contribution to the cloud albedo effect is shown to increase to $-0.37\,\mathrm{W\,m^{-2}}$ by the year 2100, if considering only the reductions in available cloud condensation nuclei. Overall, the effect of nitric acid can play a large part in aerosol cooling during the following decades with decreasing SO_2 emissions and increasing NO_x and greenhouse gases.

1 Introduction

Throughout industrialization humankind has injected increasing amounts of greenhouse gases (GHGs) into the atmosphere and thereby induced anthropogenic global warming. However, there has been a simultaneous increase in emissions of counteracting agents: aerosols and their precursors (e.g. SO_2). Aerosols alter radiative fluxes directly by scattering and absorbing radiation, and indirectly by acting as cloud condensation nuclei (CCN) and altering cloud properties (Twomey, 1977; Albrecht, 1989; Small et al., 2009). The present-day anthropogenic aerosol forcing (direct and cloud albedo effect) ranging from -0.5 to $-2.2\,\mathrm{W\,m^{-2}}$ (Forster et al., 2007) acts to cool Earth's climate, partly masking the warming from e.g. increased CO_2 concentration. The indirect aerosol effects (-0.5 to $-1.9\,\mathrm{W\,m^{-2}}$ for the cloud albedo effect, -0.3 to $-1.4\,\mathrm{W\,m^{-2}}$ for the cloud lifetime effect (Lohmann and Feichter, 2005)) are dominating the anthropogenic aerosol forcing over the direct effect ($-0.50 \pm 0.40\,\mathrm{W\,m^{-2}}$ (Forster et al., 2007)).

Anthropogenic SO_2 emissions increased from $2\,\mathrm{Tg}(SO_2)$ in year 1850 to $130\,\mathrm{Tg}(SO_2)$ in 1970's, but have already decreased about 20 % from the peak value due to emission regulations (Smith et al., 2011). In China, SO_2 emissions increased between 2000 and 2006 by 53 %, but have already

shown a decreasing trend since 2006 (Lu et al., 2010). The reductions of SO_2 emissions due to air pollution control measures can cut global emissions even by 90 % until 2100 (van Vuuren et al., 2007) which, together with reductions in primary particle emissions, would lead to a substantially weaker aerosol cooling in the future (Andreae et al., 2005; Arneth et al., 2009; Makkonen et al., 2012).

The future scenarios of NO_x emissions show generally either a stronger increase (Bauer et al., 2007; Adams et al., 2001) or a weaker decrease (Lamarque et al., 2011) than SO_2 emissions. Nitrogen oxides are formed during fuel combustion at high temperature and pressure, main sources being traffic, power generation and industry. In the IPCC scenario IS92a, annual NO_x emissions were estimated to increase substantially from 28 Tg(N) (year 2000) to 72 Tg(N) (year 2100). Later, the IPCC SRES scenarios showed a large spread in emission estimates for the year 2100 (28–151 Tg(N) yr^{-1} in the A1 scenario family). All SRES scenarios expect an increase in NO_x emissions for a few decades (until 2040–2050), following stabilization (A1 and B2 scenario families), decline (by NO_x emission control technologies and alternatives for fossil-fuel) or continued increase until 2100 (fossil-fuel intensive and high-population scenarios). The NO_x emission pathways for the next IPCC report emission scenario development (Lamarque et al., 2011) indicate a range from 16 (van Vuuren et al., 2007) to 26 (Riahi et al., 2007) Tg(N) for the year 2100, corresponding to a 30–60 % decrease in NO_x emissions from present-day levels. However, the ratio of global NO_x/SO_2 emissions is increasing throughout the 21st century (Lamarque et al., 2011).

Nitrogen oxides are precursors of nitric acid. With enough gas-phase ammonia available, ammonium nitrate can form and partition to the aerosol phase. Although the present-day aerosol load and direct forcing from nitrate aerosols is considerably smaller than from sulfate aerosols (Liao et al., 2004), the nitrate aerosols can play an important part in the future. Adams et al. (2001) estimated that the nitrate aerosol direct forcing forcing was only 20 % of the sulfate aerosol forcing in the year 2000, but with the SRES A2 future emission scenario, the nitrate forcing could be 50 % stronger than sulfate forcing in the year 2100. Bauer et al. (2007) reported an increase of nitrate forcing from -0.11 to $-0.14\,W\,m^{-2}$ from present-day to the year 2030, although this was accompanied with an increase in sulfate forcing. In Chen et al. (2010), the sulfate burden decreased slightly from 2.87 to 2.74 Tg between the years 2000 and 2100, whereas the nitrate burden quadrupled from 0.67 to 2.88 Tg.

It has been suggested that the effects of nitrogen oxides on clouds could be increasingly important with declining SO_2 emissions (Kulmala et al., 1995). Nitric acid can condense on aqueous aerosols at relative humidities (RH) close to and exceeding 100 % (Kulmala et al., 1997; Laaksonen et al., 1998; Kokkola et al., 1993). During cloud formation, RH increases relatively rapidly, and as it exceeds 100 %, the largest aerosols start activating to cloud droplets. With still increasing RH, smaller and smaller particles activate until condensation of water to already activated particles depletes water from the air, peak RH is reached, and further activation ceases, leaving still smaller particles unactivated. The activated fraction of the total aerosol can vary from less than 1 % to close to 100 %, depending on ambient conditions, and the concentration, size distribution and composition of the aerosol itself. Nitric acid influences the activation process because its condensation onto an aerosol particle increases the particle's hygroscopic mass and enables the particle to activate at lower RH. Furthermore, the acid condenses more efficiently to smaller particles with higher surface-to-volume ratio, and as a result, a larger fraction of the aerosol is able to activate (**?**Xue and Feingold, 2004). Recent ambient observations from a polluted region in China (with HNO_3 mixing ratios as high as 5 ppb) indicate that nitric acid contributes to persistent clouds which may activate even at RH's slightly below 100 % (Ma et al., 2010), which is in agreement with the earlier theoretical calculations of Kulmala et al. (1997) and Laaksonen et al. (1998). Experimental evidence of the role of HNO_3 in cloud drop formation has also been obtained by Henin et al. (2011).

Beyond nitric acid also other semi-volatile compounds affect the cloud droplet formation. It has been shown that the effect of nitric acid is enhanced by the co-condensation of ammonia, which as a base neutralizes the solution and thus condensation takes place at the lower relative humidity compared to nitric acid condensation alone (Hegg, 2000; Romakkaniemi et al., 2005a). With high enough concentrations and/or low temperatures the co-condensation leads to the formation of ammonium nitrate. However, as shown by Romakkaniemi et al. (2005b) it is difficult to estimate how much ammonia enhances activation as partitioning of ammonia and nitric acid between different sized particles is highly dependent on the air mass history. Also some organic compounds are semivolatile, and in the recent study it was shown that they also have a lot of potential to affect cloud droplet formation (Topping and McFiggans, 2012).

We study the effect of nitric acid condensation on cloud droplet activation with a global climate model, and show the importance of nitric acid on the present-day indirect forcing. We also explore how the effect can change with projected decreases in particle number concentrations.

2 Methods

2.1 Global aerosol-climate model ECHAM5.5-HAM2

We use the aerosol-climate model ECHAM5.5-HAM2 (Zhang et al., 2012) extended by a two-moment cloud microphysics scheme (Lohmann et al., 2007). The model horizontal resolution is T42, corresponding to approximately 2.8° grid. We use 31 vertical levels, extending from the surface to 10 hPa. Aerosols are activated as cloud droplets with

the scheme of Abdul-Razzak and Ghan (Abdul-Razzak and Ghan, 2000; Stier et al., 2012). The updraft velocity is calculated from the grid-mean vertical velocity, turbulent kinetic energy and convectively available potential energy. The aerosol microphysics model M7 (Vignati et al., 2004) considers the dominant aerosol compounds: dust, sea salt, black carbon, particulate organic matter and sulfate. Atmospheric new particle formation is modeled with a parameterization of binary water-sulphuric acid nucleation (Vehkamäki et al., 2002). The aerosol model does not include nitrate aerosols.

The effect of nitric acid is parameterized according to Romakkaniemi et al. (2005a), based on results from a detailed numerical air parcel model. The parameterization is applied after the calculation of activated fraction without nitric acid (F_0). The parameterization calculates the activated fraction (F_x) with a certain nitric acid volume mixing ratio from the aerosol size distribution, gas phase nitric acid concentration, temperature, total pressure, updraft velocity and the activated fraction without nitric acid. The parameterization takes into account the kinetic limitations of nitric acid and water condensation, and the effect of existing aerosol solubility. The effect of nitric acid is considered only for two aerosol modes, soluble Aitken and accumulation modes. Over continents, the number concentration of coarse mode particles is relatively small. In marine conditions, coarse mode sea-salt particles decrease the effect of HNO_3 on cloud droplet number concentrations (CDNC) (Romakkaniemi et al., 2005a). The amount of nitric acid in nucleation mode can be considered negligible in all conditions as particles are very small.

Natural emissions of sea salt (Schulz et al., 2004), dust (Tegen et al., 2002) and DMS (Kettle and Andreae, 2000) are calculated online, i.e. based on model meteorology. Both eruptive (Halmer et al., 2002) and non-eruptive (Andres and Kasgnoc, 1998) volcanic sulfur emissions are included. Emissions of biogenic volatile organic compounds are prescribed monthly averages according to Guenther et al. (1995). Present-day anthropogenic aerosol and precursor emissions are taken from AeroCom emission inventory for the year 2000 (Dentener et al., 2006). For the future simulation, we apply one scenario from the "Representative Concentration Pathways" (RCPs), which are used for the emission scenario development process of IPCC AR5 (Moss et al., 2010; Lamarque et al., 2011). The selected pathway is RCP 3-PD (van Vuuren et al., 2007), which is the most optimistic one regarding emissions of SO_2, with an emission reduction of 90 % until the year 2100. Makkonen et al. (2012) have shown that the emissions of RCP 3-PD lead to a strong decrease in aerosol concentrations and the total aerosol forcing. We will only apply the aerosol and precursor emissions from the RCP 3-PD pathway: the nitric acid concentrations are for the year 2000 in all simulations.

2.2 Radiative forcing

We use two separate methods to analyze the effect of nitric acid on cloud albedo forcing and on total indirect forcing. To obtain the effect on cloud albedo, we run the ECHAM5.5-HAM2 model for 5 yr without coupling nitric acid to cloud microphysics. Instead, at each timestep we first calculate the CDNC with the Abdul-Razzak and Ghan parameterization (Abdul-Razzak and Ghan, 2000). Then, we calculate the increase in CDNC due to nitric acid, and perform the radiation calculations twice, with and without nitric acid. The instantaneous change in radiative fluxes at top-of-atmosphere is diagnosed as cloud albedo forcing. Since the nitric acid is prescribed as monthly average 3-D-fields, the variation in the cloud albedo forcing is rather small, and a 5-yr model integration is sufficient.

For the total indirect effect, two separate simulations are needed. One control simulation is done without nitric acid included. A second simulation is carried out, where the nitric acid is allowed to change the actual CDNC used in cloud microphysics. The perturbation in CDNC can then lead to changes in e.g. cloud albedo, cloud lifetime and precipitation. The total indirect effect is analyzed as the difference in the top-of-atmosphere short-wave fluxes between the two simulations. Although the overall climate is constrained by prescribed sea-surface temperatures, the coupling of nitric acid and CDNC can alter cloud fields significantly. Hence, the two simulations are integrated for 20 yr to reduce the effect of the climate model's internal variability. The latter method used to obtain the total indirect forcing is essentially equivalent to quasi-forcing or fixed-SST-forcing calculated as radiative flux perturbation (Rotstayn and Penner, 2001).

The analyzed flux perturbations correspond to changes in present-day cloud forcing when nitric acid is explicitly described in cloud activation. Since the used nitric acid fields also contain natural sources, the resulting change in radiative fluxes is not strictly the anthropogenic forcing. However, global anthropogenic NO_x emissions are almost fivefold compared to emissions from natural sources (Delmas et al., 1997), and in areas with clouds most affected by nitric acid, the influence of anthropogenic NO_x emissions is presumably even higher.

2.3 Nitric acid

The nitric acid concentration fields are prescribed monthly mean volume mixing ratios from the RETRO study calculated with the chemistry global circulation model ECHAM5_MOZ (Rast et al., 2012). The nitric acid fields are representative of the year 2000. The chemistry in the ECHAM5_MOZ is based on MOZART2 (Horowitz et al., 2003). Nitrate aerosols are not included in ECHAM5_MOZ, hence the applied nitric acid concentration includes also the aerosol-phase nitrate. This leads to an overestimation of the nitric acid concentration, especially during nighttime. All

Table 1. Acronyms and description of the experiments. In HNO3_DIAG_2000 and HNO3_DIAG_2100, the effect of HNO_3 is diagnosed during simulation, and HNO_3 does not affect modeled climate. In HNO3_FULL_2000, the coupling of HNO_3, CDNC and modeled climate is implemented.

Experiment name	Aerosol and precursor emissions	HNO_3 concentrations	Simulated years	HNO_3 effect
HNO3_DIAG_2000	AeroCom year 2000	Year 2000	5	Diagnostic
HNO3_DIAG_2100	RCP 3-PD year 2100	Year 2000	5	Diagnostic
CTRL_2000	AeroCom year 2000	Year 2000	20	Uncoupled
HNO3_2000	AeroCom year 2000	Year 2000	20	Coupled

nitrate is assumed to be gas-phase nitric acid available for condensation, although in reality some of the nitric acid could already reside in the cloud phase due to earlier cloud cycle and would not enhance further activation. We do not apply any diurnal variation to the nitric acid concentration.

Although the ECHAM5_MOZ can capture the vertical distribution of nitric acid quantitatively well, there is a rather systematic overestimation of the concentrations. Overall bias, based on 15 different campaigns, is 74 % at 500 hPa and 124 % at 900 hPa. The overestimation could be related to too high NO_x emissions, too low wet deposition, or the lack of treatment of nitrate aerosol in ECHAM5_MOZ. The applied nitric acid fields are quantitatively similar to those in Xu and Penner (2012), with global average surface concentrations of 165 pptv and 174 pptv in this study and Xu and Penner (2012), respectively. Surface HNO_3 concentrations over remote oceans are slightly higher in ECHAM5_MOZ, while Xu and Penner (2012) show generally higher concentrations over continents.

2.4 Simulation setup

The conducted experiments are shown in Table 1. In experiments HNO3_DIAG_2000 and HNO3_DIAG_2100 the effect of nitric acid on CDNC is only diagnosted, and nitric acid does not affect simulated climate. In HNO3_2000, the CDNC perturbations due to nitric acid will affect cloud properties and simulated climate, whereas in CTRL_2000, the effect of nitric acid is completely turned off.

3 Results and discussion

3.1 Nitric acid effect on activation

Figure 1 shows the distribution of activated fractions F_x and F_0 at 8 different heights between 100 and 2000 m, taken from simulations without coupling of nitric acid and cloud microphysics (HNO3_DIAG_2000). The scatter plot is generated by correlating F_x with F_0 at each model grid point at a specific height. At low altitudes (100–200 m) the activated fraction F_0 without nitric acid effect can easily reach values over 0.3, and Fig. 1 shows a large spread in the activated fraction F_x with nitric acid at these values. Nitric acid

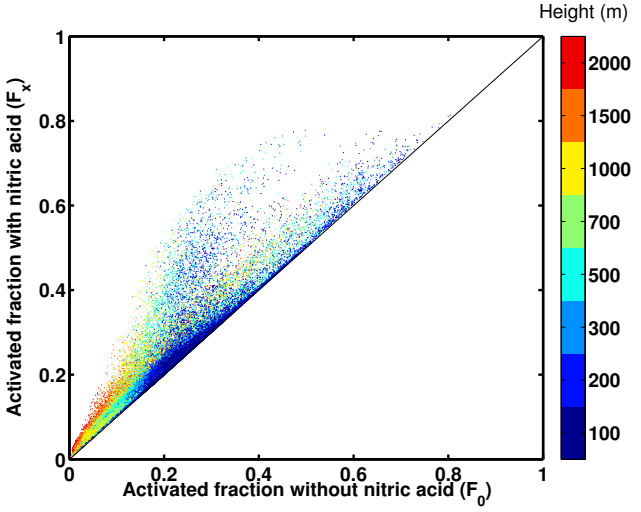

Fig. 1. Scatter plot of activated fraction with nitric acid (F_x) plotted against activated fraction without nitric acid (F_0) at 8 different heights. The scatter plots are generated by plotting 5-yr average activated fractions in each grid point against each other. The data is from simulations without coupling of nitric acid and cloud microphysics (experiment HNO3_DIAG_2000).

can not decrease the activated fraction at any point. The relative increase in activated fraction due to nitric acid increases monotonously with height, from about 10–20 % below 1 km to >50 % above 3.5 km.

The zonal distribution of CDNC increase due to nitric acid is shown in Fig. 2, calculated from experiments HNO3_2000 and CTRL_2000. The strongest effect is seen in the mid-troposphere between 500–800 hPa and between 30° S–60° N, where nitric acid can increase CDNC by more than 10 % in large areas. Figure 2 shows also the ratio of nitric acid mass versus Aitken and accumulation mode sulfate mass, indicating potential increase in nitric acid effect with height.

3.2 Present-day forcing due to nitric acid

Our simulations show a strong effect from the inclusion of nitric acid on total short-wave radiation fluxes at top-of-atmosphere: $-0.32 \pm 0.01\,W\,m^{-2}$ for the cloud albedo effect (HNO3_DIAG_2000) and $-0.46 \pm 0.26\,W\,m^{-2}$

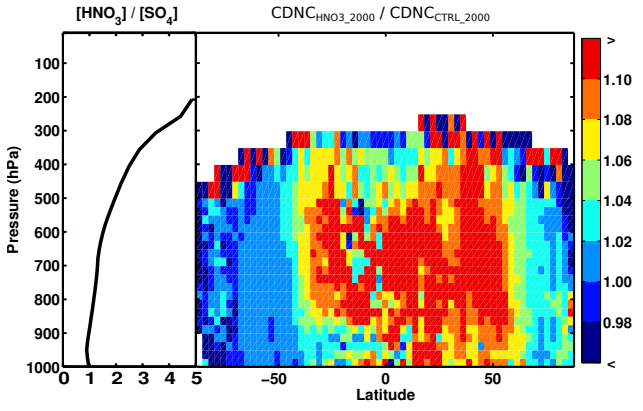

Fig. 2. Ratio of nitric acid mass vs. sulfate mass in Aitken and accumulation modes (left panel) and 20-yr zonal average ratio of CDNC between simulations with (HNO3_2000) and without (CTRL_2000) nitric acid (right panel).

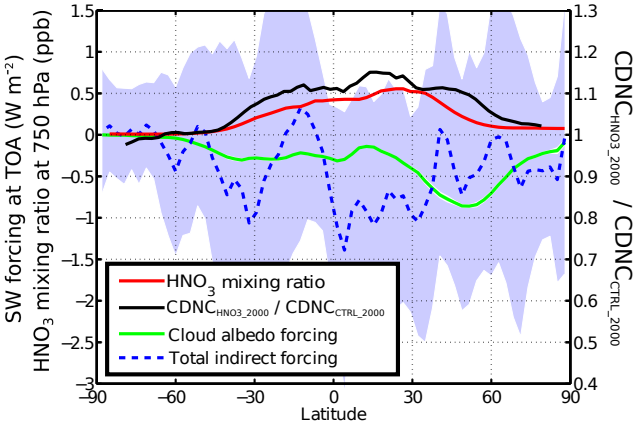

Fig. 3. Zonal average nitric acid mixing ratio at 750 hPa (ppb), cloud albedo forcing ($W\,m^{-2}$) (experiment HNO3_DIAG_2000) and total indirect forcing ($W\,m^{-2}$) due to inclusion of nitric acid. The total indirect forcing is calculated as the difference in top-of-atmosphere short-wave fluxes between experiments HNO3_2000 and CTRL_2000. Also shown is the ratio of CDNC at the 750 hPa level between experiments HNO3_2000 and CTRL_2000. The blue shading corresponds to standard deviation of the total indirect forcing. The standard deviation is presented also for the cloud albedo forcing, but it is almost indistinguishable from the green line.

($-0.42 \pm 0.28\,W\,m^{-2}$ when accounting for longwave radiation) for the total indirect effect (HNO3_2000), with the uncertainty range indicating the inter-annual standard deviation. The effect is rather large compared to the simulated anthropogenic indirect forcing without nitric acid, $-1.6\,W\,m^{-2}$.

With the NO_x sources mostly confined to the Northern Hemisphere, the cooling from nitric acid has a strong zonal pattern. Figure 3 shows the cloud albedo effect peaking between 20° N–80° N, reaching a value of $-0.90\,W\,m^{-2}$ around 50° N. The hemisphere-mean effect of nitric acid on cloud albedo forcing is $-0.17\,W\,m^{-2}$ for the Southern Hemisphere and -0.43 $W\,m^{-2}$ for the Northern Hemisphere. Similarly to the cloud albedo effect, the total indirect effect shows a strong contrast between Southern ($-0.20\,W\,m^{-2}$) and Northern ($-0.59\,W\,m^{-2}$) Hemisphere. The 5-yr global averages of the total indirect forcing extracted from the 20-yr simulation are −0.38, −0.49, −0.38 and $-0.58\,W\,m^{-2}$, so they all exceed the cloud albedo forcing of $-0.32\,W\,m^{-2}$. Figure 3 shows that the nitric acid induced perturbation to CDNC follows the nitric acid concentration, indicating that the fluctuations in total indirect effect are arising from changes in modeled cloud cover.

As shown in Fig. 4, there are differences between the spatial distributions of HNO_3 concentration and the simulated cloud albedo forcing. In addition to the nitric acid concentration, the nitric acid effect on cloud droplet concentration depends on the aerosol distribution, temperature, updraft velocity and activated fraction. The annual average HNO_3 mixing ratio at the 750 hPa level (Figure 4a) reaches >1 ppb in polluted regions (middle Africa, India, China) and is mostly between 0.1–1 ppb over continents. Although surface concentrations are even higher close to NO_x sources (annual average several ppb), the 750 hPa level shows clearly the transport of HNO_3 over oceans. The transport of HNO_3 has been observed from satellites, and HNO_3 has been suggested as a reservoir of NO_x (Wespes et al., 2007). In large parts of the North Atlantic, HNO_3 levels are between 0.3–0.5 ppb. The outflow from Africa establishes even 0.5–1 ppb of HNO_3 over the South Atlantic. The overall effect of HNO_3 on cloud droplet number concentration is largest over continents, especially over polluted regions. The cloud albedo effect ranges from −1.5 to $-2\,W\,m^{-2}$ over Eastern US, Europe, central Africa and Japan. The forcing is stronger than $-0.2\,W\,m^{-2}$ over all continental regions except for northern Africa, Middle East and Greenland. At certain locations, even a high HNO_3 concentration is not enough to produce a strong cooling: e.g. in India, the annual average HNO_3 concentration of 1 ppb or more leads to a forcing from only −0.2 to $-0.7\,W\,m^{-2}$. The cooling over India is most prominent during summer months, when the simulated aerosol concentrations are lower than average. With high enough aerosol number concentrations, the amount of nitric acid partitioned in each particle, and subsequent effect on activation, is small (Nenes et al., 2002).

The cloud albedo forcing found here, $-0.32\,W\,m^{-2}$, is slightly higher than the present-day indirect effect of $-0.23\,W\,m^{-2}$ of total nitrate and ammonium found in Xu and Penner (2012). Although the results in Xu and Penner (2012) include the contribution of particulate nitrate, the indirect effect is mainly due to gaseous nitric acid. The spatial patterns of the cloud albedo forcing are very similar. Xu and Penner (2012) show stronger forcing in Australia, continental South-East Asia, southern US and continental outflow regions, whereas the forcing found in this study is stronger in Europe, around Japan, and middle Africa. The gas-phase

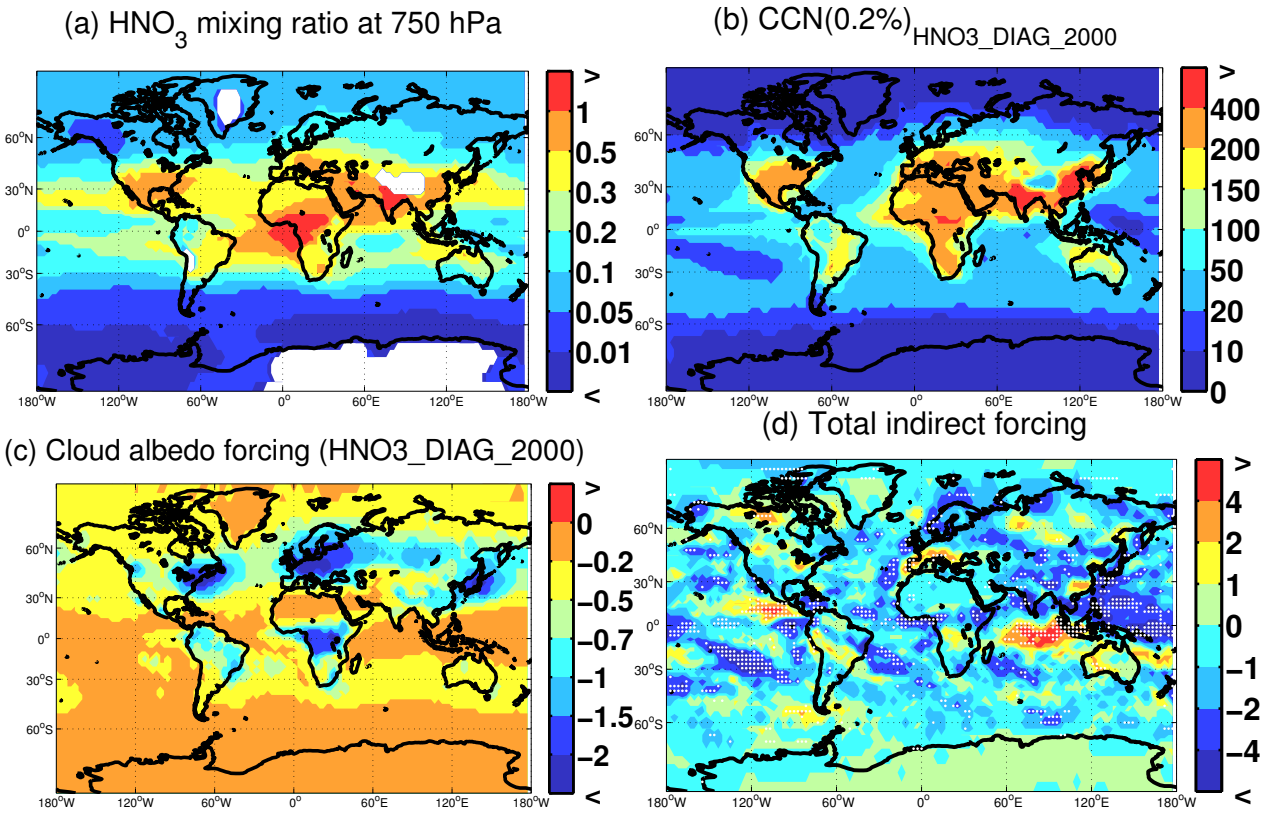

Fig. 4. **(a)** Annual average nitric acid mixing ratio at 750 hPa (ppb), **(b)** surface-level CCN(0.2 %) (cm^{-3}) from experiment HNO3_DIAG_2000 (unperturbed by nitric acid), **(c)** cloud albedo forcing ($W\,m^{-2}$) (experiment HNO3_DIAG_2000) and **(d)** total indirect forcing ($W\,m^{-2}$) due to inclusion of nitric acid, calculated from experiments HNO3_2000 and CTRL_2000. The cloud albedo forcing is averaged over 5 yr, the total indirect forcing over 20 yr. White dots in **(d)** indicate statistical significance with $p < 0.05$.

nitric acid fields used in Xu and Penner (2012) are very similar to those applied here, averaging in the surface layer of the model to 165 pptv and 174 pptv in this study and Xu and Penner (2012), respectively. The nitric acid concentrations over oceans in our study are slightly higher than those in Xu and Penner (2012).

The nitric acid inclusion leads to a global annual-mean increase of 7 % in CDNC, which is a clear signal of the nitric acid effect and sufficient for a significant cloud albedo perturbation. The CDNC increase is in good agreement with Xu and Penner (2012), where CDNC increased by 2.4 % due to particulate nitrate and 11.5 % due to total nitrate (including nitric acid effect). The zonal averages in Fig. 3 show that this CDNC increase follows the nitric acid concentration. However, the zonal averages of the total indirect forcing (Fig. 3) and especially its horizontal distribution (Fig. 4d) differ substantially from the cloud albedo effect. Indeed, Fig. 4d shows that locally, the total indirect effect can be either stronger or weaker negative than the cloud albedo effect, and even positive at many locations. The areas with positive (strong negative) total indirect forcing generally correspond to reduced (increased) cloudiness. For the most part, the changes in the horizontal distribution of cloudiness (not shown) are statistically insignificant, that is, they are undistinguishable from the internal variability of the model's climate. Thus the small-scale patterns seen in Fig. 4d are not robust. However, the nitric acid induced changes in global-mean low cloud fraction and middle cloud fraction (0.38 % and 0.40 %, respectively) are both significant at higher than 99.9 % level of confidence. This is consistent with the global-mean total indirect effect being larger than the cloud albedo effect, and provides evidence that at least in this model, nitric acid acts to increase the average cloud lifetime.

3.3 Effect of decreasing future aerosol concentration

To study the impact of decreasing aerosol concentration on the effect of nitric acid, we show results from simulations with aerosol and precursor emissions of the year 2100, but with present-day nitric acid concentrations. Low emissions of the RCP 3-PD pathway lead to a strong decrease in CCN(0.2 %) concentration (Fig. 5a and b), except for high-latitude regions. In continental Northern hemisphere, the decrease in CCN(0.2 %) concentration is generally over 50 %, while in South America, Africa and Australia the decrease is slightly smaller. More details on changing number

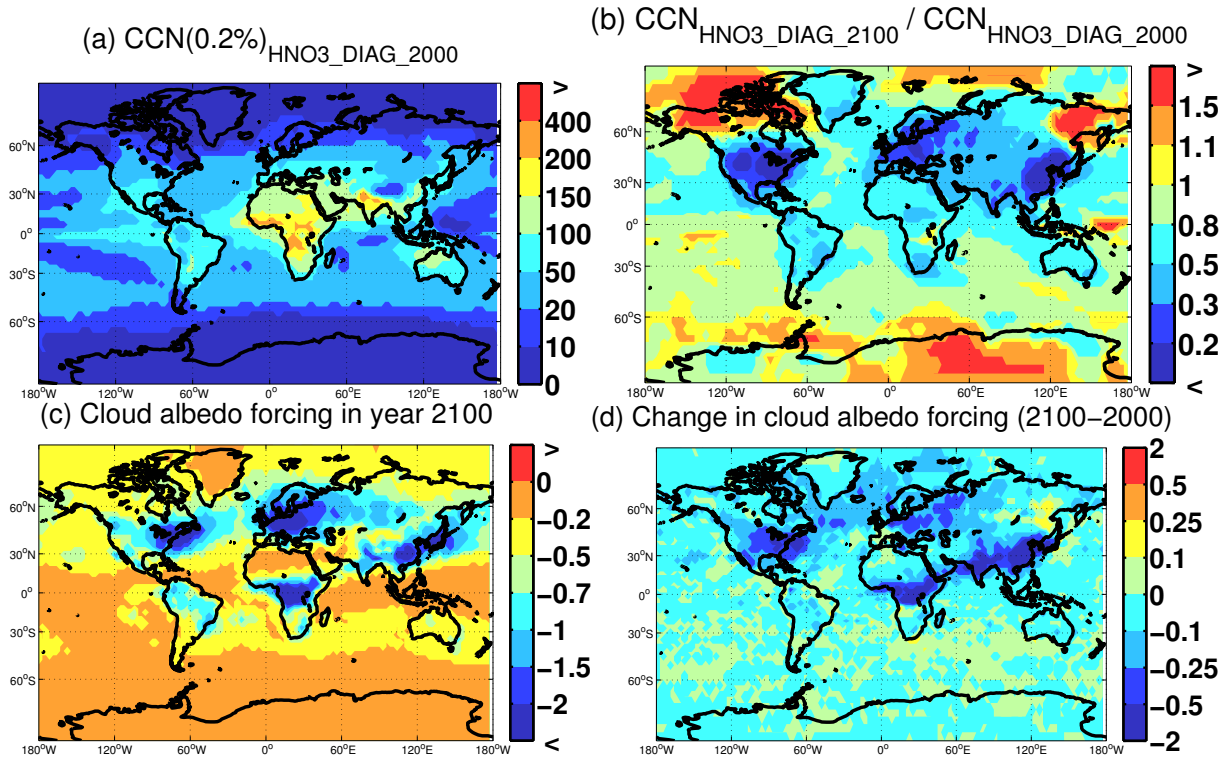

Fig. 5. **(a)** Surface-level CCN(0.2 %) (cm^{-3}) in year 2100 (HNO3_DIAG_2100), **(b)** ratio of CCN(0.2 %) between years 2100 and 2000 (experiments HNO3_DIAG_2100 and HNO3_DIAG_2000), **(c)** cloud albedo forcing ($W\,m^{-2}$) due to nitric acid in year 2100 (experiment HNO3_DIAG_2100), and **(d)** the change in cloud albedo forcing due to nitric acid ($W\,m^{-2}$) between years 2000 and 2100 (negative values indicate more cooling due to nitric acid in year 2100). The change in **(d)** is calculated as a difference of nitric acid cloud albedo forcing in experiments HNO3_DIAG_2100 and HNO3_DIAG_2000.

concentration under RCP 3-PD can be found in Makkonen et al. (2012). Note that the shown CCN concentrations are unperturbed by nitric acid.

The change in nitric acid cloud albedo forcing between years 2000 and 2100 shown in Fig. 5 is clearly connected to the change in CCN(0.2 %) concentration. The cloud albedo forcing due to nitric acid is intensified by more than $0.25\,W\,m^{-2}$ in North America, Central Africa, India, China and Eastern Europe, when moving from year 2000 to 2100. These areas show a simultaneous decrease in CCN(0.2 %) by more than 200 (cm^{-3}) (a decrease of 50–80 %). Even though the simulated present-day cloud albedo forcing can reach high values even in rather polluted areas, the results indicate that cleaning the air from particulate pollutants intensifies the nitric acid effect. The resulting negative forcing could balance the loss in aerosol forcing. The present-day global average cloud albedo effect of $-0.32\,W\,m^{-2}$ is increased to $-0.37\,W\,m^{-2}$ in the year 2100.

It should be noted that our future simulation only focused on the effect of decreasing number concentrations on the magnitude of the nitric acid effect. Also, the number concentrations are simulated with a model without nitrate aerosols, hence the anthropogenic emission changes stem only from SO_2, BC and OC. The applied nitric acid concentration is identical for years 2000 and 2100, while the RCP 3-PD shows a 60 % decrease in anthropogenic NO_x emissions (Lamarque et al., 2011). RCP 3-PD also predicts a 70 % increase in ammonia emissions, however the global ammonium aerosol burden is decreasing due to a decrease in NO_x (Lamarque et al., 2011). To fully quantify the effect of nitric acid condensation in the future aerosol forcing requires simulations with coupled aerosol-chemistry models including nitrate aerosols.

4 Conclusions

We have presented global model simulations with explicit inclusion of the effect of nitric acid condensation on cloud droplet activation. The increased soluble material increases cloud droplet number concentrations significantly, leading to a $-0.32 \pm 0.01\,W\,m^{-2}$ cloud albedo forcing and a total indirect forcing of $-0.46 \pm 0.26\,W\,m^{-2}$ with present-day emissions. While the cloud albedo effect is spatially coupled to nitric acid concentrations, the total indirect forcing is dominated by changes in low and middle cloud cover. The spatial distribution of cloud cover changes can be very much model dependent, nonetheless the total indirect effect

qualifies for an estimate for cloud effects beyond the cloud albedo effect.

We also showed that with decreasing aerosol number concentrations in the future, the effect of nitric acid could play a more important role. The applied future pathway with over 50 % reductions in CCN concentrations led to a nitric acid cloud albedo forcing of $-0.37 \pm 0.01\,\mathrm{W\,m^{-2}}$ in year 2100. While the simulation did not take into account changes in NO_x, nitrate aerosol or ammonia, it serves as indication on the effect of particle number reductions. Despite the benefits from added cooling, other environmental impacts (acid rain, ozone production) and health issues speak for reduction measures of NO_x emissions. To account for the total effect of NO_x on aerosols and clouds, one should also consider NO_x as a source of ozone.

Acknowledgements. The financial support by the Academy of Finland Centre of Excellence program (project no. 1118615) and EU-project EUCAARI (European Integrated project on Aerosol Cloud Climate and Air Quality interactions, project no. 036833-2) is gratefully acknowledged. We thank the Finnish IT center for science (CSC) for technical support and computing time. M. Kulmala acknowledges support from the European Research Council Advanced Grant (no. 227463). S. Romakkaniemi has been supported by the strategic funding of the University of Eastern Finland. P. Räisänen acknowledges support from the Academy of Finland (project no. 127210). We are grateful to the two anonymous reviewers for their valuable comments and suggestions.

Edited by: C. Hoose

References

Abdul-Razzak, H. and Ghan, S. J.: A parameterization of aerosol activation – 2: Multiple aerosol types, J. Geophys. Res., 105, 6837–6844, 2000.

Adams, P., Seinfeld, J., Koch, D., Mickley, L., and Jacob, D.: General circulation model assessment of direct radiative forcing by the sulfate-nitrate-ammonium-water inorganic aerosol system, J. Geophys. Res., 106, 1097, doi:10.1029/2000JD900512, 2001.

Albrecht, B. A.: Aerosol, cloud microphysics, and fractional cloudiness, Science, 245, 1227–1230, 1989.

Andreae, M., Jones, C., and Cox, P.: Strong present-day cooling implies a hot future, Nature, 435, 1187–1190, 2005.

Andres, R. J. and Kasgnoc, A. D.: A time-averaged inventory of subaerial volcanic sulfur emissions, J. Geophys. Res. D: Atmos., 103, 25251–25261, doi:10.1029/98JD02091, 1998.

Arneth, A., Unger, N., Kulmala, M., and Andreae, M. O.: Clean the Air, Heat the Planet?, Science, 326, 672–673, doi:10.1126/science.1181568, 2009.

Bauer, S. E., Koch, D., Unger, N., Metzger, S. M., Shindell, D. T., and Streets, D. G.: Nitrate aerosols today and in 2030: a global simulation including aerosols and tropospheric ozone, Atmos. Chem. Phys., 7, 5043–5059, doi:10.5194/acp-7-5043-2007, 2007.

Chen, W.-T., Lee, Y., Adams, P., Nenes, A., and Seinfeld, J.: Will black carbon mitigation dampen aerosol indirect forcing?, Geophys. Res. Lett., 37, L09801, doi:10.1029/2010GL042886, 2010.

Delmas, R., Serça, D., and Jambert, C.: Global inventory of NOx sources, Nutr. Cycl. Agroecosys., 48, 51–60, doi:10.1023/A:1009793806086, 1997.

Dentener, F., Kinne, S., Bond, T., Boucher, O., Cofala, J., Generoso, S., Ginoux, P., Gong, S., Hoelzemann, J. J., Ito, A., Marelli, L., Penner, J. E., Putaud, J.-P., Textor, C., Schulz, M., van der Werf, G. R., and Wilson, J.: Emissions of primary aerosol and precursor gases in the years 2000 and 1750 prescribed data-sets for AeroCom, Atmos. Chem. Phys., 6, 4321–4344, doi:10.5194/acp-6-4321-2006, 2006.

Forster, P., Ramaswamy, V., Artaxo, P., Berntsen, T., Betts, R., Fahey, D. W., Haywood, J., Lean, J., Lowe, D. C., Myhre, G., Nganga, J., Prinn, R., Raga, G., Schulz, M., and Van Dorland, R.: Climate Change 2007, The Physical Science Basis, Contribution of Working Group I to the Fourth Assessment Report of the Intergovernmental Panel on Climate Change, Cambridge Univ. Press, Cambridge, UK, and New York, NY, USA, 2007.

Guenther, A., Hewitt, C. N., Ericson, D., Fall, R., Geron, C., Graedel, T., Harley, P., Klinger, R., Lerdau, M., McKay, W. A., Pierce, T., Scholes, R., Steinbrecher, R., Tallamraju, R., Taylor, J., and Zimmerman, P.: A model of natural volatile organic compound emissions, J. Geophys. Res., 100, 8873–8892, 1995.

Halmer, M. M., Schmincke, H. U., and Graf, H. F.: The annual volcanic gas input into the atmosphere, in particular into the stratosphere: A global data set for the past 100 years, J. Volcanol Geoth. Res., 115, 511–528, doi:10.1016/S0377-0273(01)00318-3, 2002.

Hegg, D. A.: Impact of gas-phase HNO_3 and NH_3 on microphysical processes in atmospheric clouds, Geophys. Res. Lett., 27, 2201–2204, doi:10.1029/1999GL011252, 2000.

Henin, S., Petit, Y., Rohwetter, P., Stelmaszczyk, K., Hao, Z., Nakaema, W., Vogel, A., Pohl, T., Schneider, F., Kasparian, J., Weber, K., Wöste, L., and Wolf, J.-P.: Field measurements suggest the mechanism of laser-assisted water condensation, Nat. Commun., 2, 456, doi:10.1038/ncomms1462, 2011.

Horowitz, L., Walters, S., Mauzerall, D., Emmons, L., Rasch, P., Granier, C., Tie, X., Lamarque, J., Schultz, M., Tyndall, G., Orlando, J., and Brasseur, G.: A global simulation of tropospheric ozone and related tracers: Description and evaluation of MOZART, version 2, J. Geophys. Res. D: Atmos., 108, ACH 16-1–ACH 16-25, 2003.

Kettle, A. and Andreae, M.: Flux of the dimethylsulfide from the oceans: A comparison of updated data sets and flux models, J. Geophys. Res., 105, 26793–26808, doi:10.1029/2000JD900252, 2000.

Kulmala, M., Laaksonen, A., Korhonen, P., Vesala, T., Ahonen, T., and Barrett, J. C.: The effect of atmospheric nitric acid vapor on CCN activation, J. Geophys. Res., 98, 22949–22958, 1993.

Kulmala, M., Korhonen, P., Laaksonen, A., and Vesala, T.: Changes in cloud properties due to NO_x emissions, Geophys. Res. Lett., 22, 239–242, 1995.

Kulmala, M., Laaksonen, A., Charlson, R. J., and Korhonen, P.: Clouds without supersaturation, Nature, 338, 336–337, 1997.

Laaksonen, A., Korhonen, P., Kulmala, M., and Charlson, R.: Modification of the Köhler Equation to Include Soluble Trace Gases and Slightly Soluble Substance, J. Atmos. Sci., 55, 853–862,

1998.

Lamarque, J.-F., Kyle, G., Meinshausen, M., Riahi, K., Smith, S., van Vuuren, D., Conley, A., and Vitt, F.: Global and regional evolution of short-lived radiatively-active gases and aerosols in the Representative Concentration Pathways, Clim. Change, 109, 191–212, doi:10.1007/s10584-011-0155-0, 2011.

Liao, H., Seinfeld, J., Adams, P., and Mickley, L.: Global radiative forcing of coupled tropospheric ozone and aerosols in a unified general circulation model, J. Geophys. Res. D: Atmos., 109, D16207 1–33, doi:10.1029/2003JD004456, 2004.

Lohmann, U. and Feichter, J.: Global indirect aerosol effects: a review, Atmos. Chem. Phys., 5, 715–737, doi:10.5194/acp-5-715-2005, 2005.

Lohmann, U., Stier, P., Hoose, C., Ferrachat, S., Kloster, S., Roeckner, E., and Zhang, J.: Cloud microphysics and aerosol indirect effects in the global climate model ECHAM5-HAM, Atmos. Chem. Phys., 7, 3425–3446, doi:10.5194/acp-7-3425-2007, 2007.

Lu, Z., Streets, D. G., Zhang, Q., Wang, S., Carmichael, G. R., Cheng, Y. F., Wei, C., Chin, M., Diehl, T., and Tan, Q.: Sulfur dioxide emissions in China and sulfur trends in East Asia since 2000, Atmos. Chem. Phys., 10, 6311–6331, doi:10.5194/acp-10-6311-2010, 2010.

Ma, J., Chen, Y., Wang, W. Yan, P., Liu, H., Yang, S., Hu, Z., and Lelieveld, J.: Strong air pollution causes widespread haze-clouds over China, J. Geophys. Res., 115, D18204, doi:10.1029/2009JD013065, 2010.

Makkonen, R., Asmi, A., Kerminen, V.-M., Boy, M., Arneth, A., Hari, P., and Kulmala, M.: Air pollution control and decreasing new particle formation lead to strong climate warming, Atmos. Chem. Phys., 12, 1515–1524, doi:10.5194/acp-12-1515-2012, 2012.

Moss, R. H., Edmonds, J. A., Hibbard, K. A., Manning, M. R., Rose, S. K., van Vuuren, D. P., Carter, T. R., Emori, S., Kainuma, M., Kram, T., Meehl, G. A., Mitchell, J. F. B., Nakicenovic, N., Riahi, K., Smith, S. J., Stouffer, R. J., Thomson, A. M., Weyant, J. P., and Wilbanks, T. J.: The next generation of scenarios for climate change research and assessment, Nature, 463, 747–756, doi:10.1038/nature08823, 2010.

Nenes, A., Charlson, R. J., Facchini, M. C., Kulmala, M., Laaksonen, A., and Seinfeld, J. H.: Can chemical effects on cloud droplet number rival the first indirect effect, Geophys. Res. Lett., 29, 1848, doi:10.1029/2002GL015295, 2002.

Rast, S. et al.: Evaluation of the tropospheric chemistry general circulation model ECHAM5-MOZ and its application to the analysis of the chemical composition of the troposphere for the period 1960-2000 (RETRO), Max Plank Institute report, No. 114, Hamburg, Germany, 2012.

Riahi, K., Gruebler, A., and Nakicenovic, N.: Scenarios of long-term socio-economic and environmental development under climate stabilization, Technol. Forecast. Soc., 74, 887–935, doi:10.1016/j.techfore.2006.05.026, 2007.

Romakkaniemi, S., Kokkola, H., and Laaksonen, A.: Parameterization of the nitric acid effect on CCN activation, Atmos. Chem. Phys., 5, 879–885, doi:10.5194/acp-5-879-2005, 2005a.

Romakkaniemi, S., Kokkola, H., and Laaksonen, A.: The soluble trace gas effect on CCN activation: infuence of initial equilibration on cloud model results. J. Geophys. Res. 110, D15202, doi:10.1029/2004JD005364, 2005b.

Rotstayn, L. and Penner, J.: Indirect aerosol forcing, quasi forcing, and climate response, J. Climate, 14, 2960–2975, 2001.

Schulz, M., de Leeuw, G., and Balkanski, Y.: Sea-salt aerosol source functions and emissions, in Emission of Atmospheric Trace Compounds, 333–359, 2004.

Small, J. D., Chuang, P. Y., Feingold, G., and Jiang, H.: Can aerosol decrease cloud lifetime?, Geophys. Res. Lett., 36, L16806, doi:10.1029/2009GL038888, 2009.

Smith, S. J., van Aardenne, J., Klimont, Z., Andres, R. J., Volke, A., and Delgado Arias, S.: Anthropogenic sulfur dioxide emissions: 1850–2005, Atmos. Chem. Phys., 11, 1101–1116, doi:10.5194/acp-11-1101-2011, 2011.

Stier, P. et al.: Mechanistic Aerosol-Cloud Coupling and Indirect Aerosol Effects in the aerosol-climate model ECHAM-HAM, in preparation, 2012.

Tegen, I., Harrison, S. P., Kohfeld, K., Prentice, I. C., Coe, M., and Heimann, M.: Impact of vegetation and preferential source areas on global dust aerosol: Results from a model study, J. Geophys. Res., 107, 4576, doi:10.1029/2001JD000963, 2002.

Topping, D. O. and McFiggans, G.: Tight coupling of particle size, number and composition in atmospheric cloud droplet activation, Atmos. Chem. Phys., 12, 3253–3260, doi:10.5194/acp-12-3253-2012, 2012.

Twomey, S.: The influence of pollution on the shortwave albedo of clouds, J. Atmos. Sci., 34, 1149–1152, 1977.

van Vuuren, D. P., den Elzen, M. G. J., Lucas, P. L., Eickhout, B., Strengers, B. J., van Ruijven, B., and Wonink, S. van Houdt, R.: Stabilizing greenhouse gas concentrations at low levels: an assessment of reduction strategies and costs, Clim. Change, 81, 119–159, doi:10.1007/s/10584-006-9172-9, 2007.

Vehkamäki, H., Kulmala, M., Napari, I., Lehtinen, K. E. J., Timmreck, C., Noppel, M., and Laaksonen, A.: An improved parameterization for sulfuric acid/water nucleation rates for tropospheric and stratospheric conditions, J. Geophys. Res., 107, 4622–4631, 2002.

Vignati, E., Wilson, J., and Stier, P.: M7: An efficient size-resolved aerosol microphysics module for large-scale aerosol transport models, J. Geophys. Res., 109, D22202, doi:10.1029/2003JD004485, 2004.

Wespes, C., Hurtmans, D., Herbin, H., Barret, B., Turquety, S., Hadji-Lazaro, J., Clerbaux, C., and Coheur, P.-F.: First global distributions of nitric acid in the troposphere and the stratosphere derived from infrared satellite measurements, J. Geophys. Res., 112, D13311, doi:10.1029/2006JD008202, 2007.

Xu, L. and Penner, J. E.: Global simulations of nitrate and ammonium aerosols and their radiative effects, Atmos. Chem. Phys. Discuss., 12, 10115–10179, doi:10.5194/acpd-12-10115-2012, 2012.

Xue, H. and Feingold, G.: A modeling study of the effect of nitric acid on cloud properties, J. Geophys. Res., 109, D18204, doi:10.1029/2004JD004750, 2004.

Zhang, K., O'Donnell, D., Kazil, J., Stier, P., Kinne, S., Lohmann, U., Ferrachat, S., Croft, B., Quaas, J., Wan, H., Rast, S., and Feichter, J.: The global aerosol-climate model ECHAM-HAM, version 2: sensitivity to improvements in process representations, Atmos. Chem. Phys. Discuss., 12, 7545–7615, doi:10.5194/acpd-12-7545-2012, 2012.